Highly Efficient Metal-Free Growth of Nitrogen-Doped Single-Walled Carbon Nanotubes on Plasma-Etched Substrates for Oxygen Reduction

Dingshan Yu,[†] Qiang Zhang,[†] and Liming Dai*

Department of Chemical Engineering, Case Western Reserve University, Cleveland, Ohio 44106

Received June 26, 2010; E-mail: liming.dai@case.edu

Abstract: We have for the first time developed a simple plasma-etching technology to effectively generate metal-free particle catalysts for efficient metal-free growth of undoped and/or nitrogen-doped single-walled carbon nanotubes (CNTs). Compared with undoped CNTs, the newly produced metal-free nitrogen-containing CNTs were demonstrated to show relatively good electrocatalytic activity and long-term stability toward oxygen reduction reaction (ORR) in an acidic medium. Owing to the highly generic nature of the plasma etching technique, the methodology developed in this study can be applied to many other substrates for efficient growth of metal-free CNTs for various applications, ranging from energy related to electronic and to biomedical systems.

The metal residuals from metal nanoparticles used as catalysts for the conventional CNT growth often cause detrimental effects undesirable for various applications, including electronic and biological systems.[1] The recent discovery of metal-free growth of carbon nanotubes (CNTs) has offered an alternative approach to carbon nanomaterials with novel properties attractive for many existing and new applications.[2,3] Along with the recent intensive research efforts in reducing or replacing the Pt-based electrode in fuel cells,[4] Gong et al.[5] have recently found that vertically aligned nitrogen-containing carbon nanotubes (VA-NCNTs) could act as extremely effective metal-free electrocatalysts for the oxygen reduction reaction (ORR), a key factor to limiting the performance of a fuel cell. The metal-free VA-NCNTs were shown to catalyze an efficient four-electron ORR process free from CO "poisoning" with a much higher electrocatalytic activity and better long-term operation stability than those of commercially available Pt-based electrodes in alkaline electrolytes.[5] This finding has a large impact on the fuel cell field and the catalyst community, and its repercussions are continuing.[6] However, the CNTs used in the previous report[5] were produced by pyrolysis of iron(II) phthalocyanine (a metal heterocyclic molecule containing nitrogen)[7] with the residual Fe catalyst particles being removed by electrochemical oxidation. Although great care was taken during the nanotube electropurification and similar ORR electrocatalytic performance has also been reported for nitrogen-doped ordered mesoporous graphitic arrays prepared by a metal-free nanocasting technology,[6h] possible effects of metal contaminates in the NCNTs on the observed superb ORR performance could still be a matter of controversy,[8,9] unless NCNTs with good ORR electrocatalytic activities can be produced by a metal-free preparation procedure. In this regard, it will be a significant advancement if we can develop a metal-free growth process to produce NCNTs for the ORR and other applications. As far as we are aware, however, no NCNT has been produced by the metal-free growth and possible use of nitrogen-free CNTs produced by the metal-free growth has also been largely precluded by its low growth efficiency.[2,3]

Here, we report a simple but effective approach to the growth of densely packed undoped and/or nitrogen-doped single-walled carbon nanotubes from metal-free nanoparticles produced by water-plasma etching[10a] SiO$_2$/Si wafers. The resultant NCNTs were demonstrated to show considerably higher ORR electrocatalytic activities than undoped CNTs in both alkaline and acidic media. This is the first time for the plasma technology to be used to generate metal-free particles for effectively catalyzing the CNT growth and the first growth of NCNTs by the metal-free process as efficient ORR electrocatalysts under acidic conditions. Although most recent studies on the ORR by N-doped carbon nanostructures focused on alkaline electrolytes, fuel cells that operate with acidic electrolytes (particularly the proton exchange membrane fuel cell, PEMFC) could have a more significant economic impact.

Figure 1 shows a schematic representation of the nanotube synthesis procedure. Typically, a SiO$_2$/Si wafer with a 30-nm-thick SiO$_2$ coating was water-plasma etched at 30 W, 250 kHz, and 0.62 Torr for 20 min[10a] to produce SiO$_2$ nanoparticles as the metal-free catalysts on the substrate. The plasma etched substrate was then placed into a tube furnace for the metal-free growth of CNTs by chemical vapor deposition (CVD) (Figure 1).
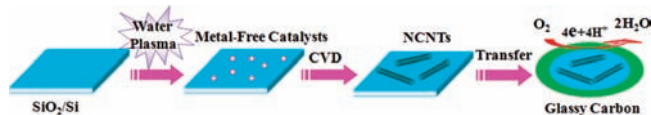

Figure 1. Metal-free growth of nitrogen-doped CNTs for the ORR.

As shown in Figures 2a and b and S1, atomic force microscope (AFM) imaging of the water-plasma etched SiO$_2$/Si substrate clearly shows the formation of homogenously distributed catalyst particles with an average size of <5 nm. The particle density was estimated to be ∼150 particles/μm^2. Prior to the nanotube deposition, X-ray photoelectron spectroscopy (XPS) was used to confirm that the water-plasma-induced nanoparticles, with and without HNO$_3$ washing (Supporting Information), are free from metal (Figures S2−S7). The metal-free SiO$_2$ nanoparticles were demonstrated to effectively support the growth of CNTs under a mixture flow of 100 sccm CH$_4$ and 100 sccm H$_2$ at 900 °C for 20 min (Figure 2c). Similarly, it was found that CNTs can also effectively grow on water-plasma-etched quartz and mica surfaces (Figures S8−S11), indicating the versatility of plasma etching for creating high density metal-free catalyst particles on various substrates. By introducing 50 sccm NH$_3$ during the metal-free CVD process, densely packed NCNTs were produced on the water-plasma-etched SiO$_2$/Si substrate (Figures 2d). In contrast, no nanotube deposition was seen for the pristine SiO$_2$/Si wafer under the same conditions. High-resolution transmission
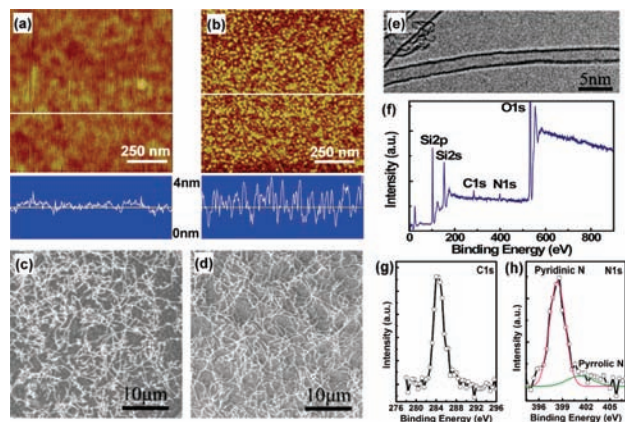
Figure 2. AFM images of the SiO₂/Si surface (a) before and (b) after the water-plasma treatment. SEM images of (c) undoped and (d) N-doped CNTs grown on the water-plasma-treated SiO₂/Si substrates. (e) HRTEM image, (f) XPS survey, (g) XPS C1s, and (h) XPS N1s spectra of the N-doped CNTs.

electron microscopy (HRTEM) observation reveals single-wall characteristics (Figures 2e and S6), which was further supported by Raman spectra showing the radial breathing modes (RBM) of SWCNTs (Figure S12). The RBM peaks at 150.7, 170.0, 179.6, and 192.7 cm^{-1} correspond to the nanotube diameters 1.65, 1.46, 1.38, and 1.29 nm, respectively,[11] largely consistent with the electron microscopic observation. The corresponding XPS spectra (Figures 2f−h and S3) clearly indicate the absence of any metal element for either CNTs or NCNTs produced by the metal-free growth. The XPS N1s spectrum for the NCNTs (3.6 at.% N), together with the curve fitting, given in Figure 2h reveals two peaks at about 401 and 398 eV attributable to the pyrrolic-like (17%) and pyridinic-like (83%) nitrogen, respectively, with the pyridine nitrogen being dominant. This is an additional advantage for the metal-free NCNTs to be used for the ORR as the pyridinic group has been shown to be more active than its pyrrolic counterpart.[9]

For the ORR measurements, the *as-synthesized* NCNTs were transferred onto a glassy carbon (GC) electrode (Supporting Information). As seen in Figure 3a, the NCNT/GC electrode shows a substantial reduction process at about 0.2 V in the presence of oxygen, while no obvious response was observed at the same potential range under N₂. Compared to CNTs, the ORR onset potential for the NCNTs shifted to a more positive value with a considerably higher electrocatalytic activity (Figure 3b), consistent with the previous report on vertically aligned carbon nanotubes produced by the metal-catalytic growth.[5] Owing to the metal-free growth, the observed electrocatalytic activity toward the ORR for the newly produced NCNTs could be attributed exclusively to the incorporation of nitrogen in the CNT structure.

As is the case with the VA-NCNTs,[5] we can attribute the improved catalytic performance observed for the metal-free NCNTs produced in the present study to the electron-accepting ability of the nitrogen atoms, which creates net positive charge on adjacent carbon atoms in the nanotube structure to readily attract electrons from the anode for facilitating the ORR. Considering that the N content (3.6 at.%) in the present metal-free NCNTs is rather moderate, further improvement in the ORR activity can be achieved by optimizing the metal-free growth conditions to regulate the N content and the respective percentage of the pyridinic and pyrrolic nitrogen groups.[6h,9]

To explore the oxygen reduction reaction in a more quantitative manner, the transferred electron number per oxygen molecule
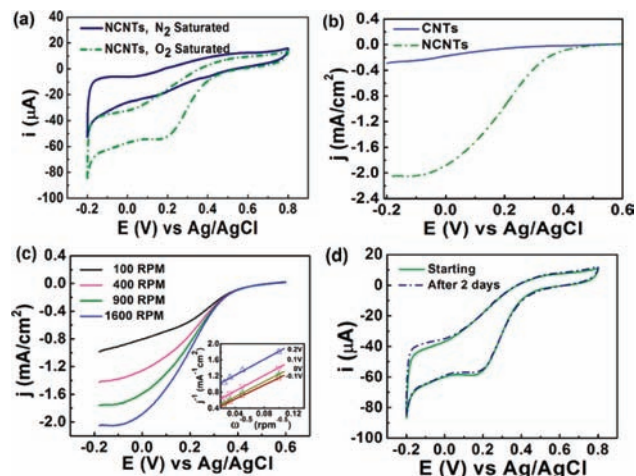

Figure 3. (a) Cyclic voltammograms of the NCNTs at a scan rate of 50 mV/s in 0.5 M H₂SO₄ solution saturated with N₂ or O₂. (b) Rotating-disk-electrode (RDE) linear sweep voltammograms of the NCNTs and undoped CNTs in oxygen-saturated 0.5 M H₂SO₄ at a scan rate of 10 mV/s. (c) RDE curves of the NCNT in oxygen-saturated 0.5 M H₂SO₄ with different speeds of 100, 400, 900, and 1600 rpm at a scan rate of 10 mV/s (the inset showing the Koutecky−Levich plots of the NCNT derived from RDE measurements). (d) Electrochemical stability measurements of the NCNT by using continuous cyclic voltammetry in oxygen-saturated 0.5 M H₂SO₄ at a scan rate of 50 mV/s.

Table 1. Kinetic Current (j_k) and Average Number of Electrons Transferred for Oxygen Reduction (n_i) at Different Potentials for NCNTs in Oxygen-Saturated 0.5 M H₂SO₄

i	E_i (V) vs Ag/AgCl	j_k (mA/cm²)	n_i
1	−0.10	3.54	3.92
2	0	3.19	3.71
3	0.10	2.25	3.60
4	0.20	1.20	3.52

involved in the ORR process was further determined by the Koutecky−Levich equation,[12] which relates the current density j to the rotation rate of the electrode ω:

$$\frac{1}{j} = \frac{1}{j_k} + \frac{1}{B\omega^{0.5}} \tag{1}$$

where j_k is the kinetic current density and B is related to the diffusion-limiting current density expressed by the following expression:

$$B = 0.2nF(D_{O_2})^{2/3}v^{-1/6}C_{O_2} \tag{2}$$

The Koutecky−Levich curves were plotted for different potentials in the inset of Figure 3c. The parallel and straight fitting lines of $1/j$ *vs* $1/\omega^{0.5}$ imply a first-order reaction toward dissolved oxygen. The n value for the NCNTs is derived to be 3.52−3.92 at the potential ranging from −0.1 to 0.2 V, suggesting a four-electron process for the ORR on the NCNT electrode (Table 1). This is further confirmed by the negligible ring current recorded at a Pt rotating ring-disk electrode (RRDE) (Figure S13).[5,6i] We have also investigated the electrochemical stability of the NCNT electrode for the ORR in O₂-saturated 0.5 M H₂SO₄ for 2 days using cyclic voltammetry. The continuous potential cycling did not cause any loss of the specific catalytic activity for the NCNT electrode (Figure 3d), indicating that the catalytic sites of the NCNT are rather stable in an acidic medium.

In summary, we have developed a simple, but effective and versatile, plasma-etching technology to generate metal-free particle catalysts for efficient metal-free growth of CNTs. Compared with undoped CNTs, the newly produced metal-free NCNTs were demonstrated to show relatively good electrocatalytic activity and long-term stability toward the ORR in an acidic medium. Owing to the highly generic nature of the plasma etching technique, the methodology developed in this study can be applied to many other substrates for efficient growth of metal-free carbon nanotubes useful for various applications, ranging from energy related to electronic and to biomedical systems.

Supporting Information Available: Detailed experimental, SEM, TEM, XPS, and electrochemical test results. This material is available free of charge via the Internet at http://pubs.acs.org.

References

(1) (a) Dai, L., Ed. *Carbon Nanotechnology: Recent Developments in Chemistry, Physics, Materials Science and Device Applications*; Elsevier: Amsterdam, 2006. (b) Isobe, H.; Tanaka, T.; Maeda, R.; Noiri, E.; Solin, N.; Yudasaka, M.; Iijima, S.; Nakamura, E. *Angew. Chem., Int. Ed.* **2006**, *45*, 6676–6680. (c) Liua, X.; Guob, L.; Morrisb, D.; Kanec, A. B.; Hurtb, R. H. *Carbon* **2008**, *46*, 489–500.
(2) (a) Liu, B. L.; Ren, W. C.; Gao, L. B.; Li, S. S.; Pei, S. F.; Liu, C.; Jiang, C. B.; Cheng, H. M. *J. Am. Chem. Soc.* **2009**, *131*, 2082–2083. (b) Huang, S. M.; Cai, Q. R.; Chen, J. Y.; Qian, Y.; Zhang, L. J. *J. Am. Chem. Soc.* **2009**, *131*, 2094–2095.
(3) (a) Liu, B. L.; Ren, W. C.; Liu, C.; Sun, C. H.; Gao, L. B.; Li, S. S.; Jiang, C. B.; Cheng, H. M. *ACS Nano* **2009**, *3*, 3421–3430. (b) Rao, F. B.; Li, T.; Wang, Y. *Carbon* **2009**, *47*, 3580–3584. (c) Liu, H. P.; Takagi, D.; Chiashi, S.; Homma, Y. *Carbon* **2010**, *48*, 114–122. (d) Homma, Y.; Liu, H. P.; Takagi, D.; Kobayashi, Y. *Nano Res.* **2009**, *2*, 793–799. (e) Gao, F. L.; Zhang, L. J.; Huang, S. M. *Appl. Surf. Sci.* **2010**, *256*, 2323–2326. (f) Takagi, D.; Kobayashi, Y.; Hommam, Y. *J. Am. Chem. Soc.* **2009**, *131*, 6922–6923. (g) Steiner, S. A.; Baumann, T. F.; Bayer, B. C.; Blume, R.; Worsley, M. A.; MoberlyChan, W. J.; Shaw, E. L.; Schlogl, R.; Hart, A. J.; Hofmann, S.; Wardle, B. L. *J. Am. Chem. Soc.* **2009**, *131*, 12144–12154.
(4) (a) Charreteur, F.; Jaouen, F.; Ruggeri, S.; Dodelet, J. *Electrochim. Acta* **2008**, *53*, 2925–2938. (b) Lefèvre, M.; Proietti, E.; Jaouen, F.; Dodelet, J. *Science* **2009**, *324*, 71–74.
(5) Gong, K. P.; Du, F.; Xia, Z. H.; Durstock, M.; Dai, L. M. *Science* **2009**, *323*, 760–764.
(6) (a) Lyth, S. M.; Nabae, Y.; Moriya, S.; Kuroki, S.; Kakimoto, M.; Ozaki, J.; Miyata, S. *J. Phys. Chem. C* **2009**, *113*, 20148–20151. (b) Chen, Z.; Higgins, D.; Tao, H. S.; Hsu, R. S.; Chen, Z. W. *J. Phys. Chem. C* **2009**, *113*, 21008–21013. (c) Tang, Y. F.; Allen, B. L.; Kauffman, D. R.; Star, A. *J. Am. Chem. Soc.* **2009**, *131*, 13200–13201. (d) Qu, L.; Liu, Y.; Baek, J.-B.; Dai, L. *ACS Nano* **2010**, *4*, 1321–1326. (e) Jin, C.; Nagaiah, T. C.; Xia, W.; Spliethoff, B.; Wang, S.; Bron, M.; Schuhmann, W.; Muhler, M. *Nanoscale* **2010**, *2*, 981–987. (f) Ozaki, J.; Tanifuji, S.; Furuichi, A.; Yabutsuka, K. *Electrochim. Acta* **2010**, *55*, 1864–1871. (g) Wang, X.; Lee, J. S.; Zhu, Q.; Liu, J.; Wang, Y.; Dai, S. *Chem. Mater.* **2010**, *22*, 2178–2180. (h) Liu, R.; Wu, D.; Feng, X.; Müllen, K. *Angew. Chem., Int. Ed.* **2010**, *(49)*, 2565–2569. (i) Xu, X.; Jiang, S.; Hu, Z.; Liu, S. *ACS Nano* **2010**, *(4)*, 4292–4298. (j) Jiang, S.; Ma, Y.; Jian, G.; Tao, H.; Wang, X.; Fan, Y.; Lu, Y.; Hu, Z.; Chen, Y. *Adv. Mater.* **2009**, *21*, 4953–4956. (k) Liu, G.; Li, X.; Ganesan, P.; Popov, B. N. *Electrochim. Acta* **2010**, *55*, 2853–2858. (l) Liu, G.; Li, X.; Ganesan, P.; Popov, B. N. *Appl. Catal., B* **2009**, *93*, 156–165. (m) Numerous refereed papers have cited the Science paper (*i.e.*, ref 5) just within about one year after its publication; see, for example, ISI Web of KnowledgeSM.
(7) (a) Huang, S. M.; Dai, L. M.; Mau, A. W. H. *J. Phys. Chem. B* **1999**, *103*, 4223–4227. (b) Huang, S. M.; Dai, L. M.; Mau, A. W. H. *Adv. Mater.* **2002**, *14*, 1140.
(8) (a) Lefevre, M.; Proietti, E.; Jaouen, F.; Dodelet, J. P. *Science* **2009**, *324*, 71–74. (b) Yang, J. B.; Liu, D. J.; Kariuki, N. N.; Chen, L. X. *Chem. Commun.* **2008**, 329–331. (c) Titov, A.; Zapol, P.; Kral, P.; Liu, D. J.; Iddir, H.; Baishya, K.; Curtiss, L. A. *J. Phys. Chem. C* **2009**, *113*, 21629–21634.
(9) Kundu, S.; Nagaiah, T. C.; Xia, W.; Wang, Y. M.; Van Dommele, S.; Bitter, J. H.; Santa, M.; Grundmeier, G.; Bron, M.; Schuhmann, W.; Muhler, M. *J. Phys. Chem. C* **2009**, *113*, 14302–14310.
(10) (a) Dai, L. M.; Griesser, H. J.; Mau, A. W. H. *J. Phys. Chem. B* **1997**, *101*, 9548–9554. (b) Chen, Q. D.; Dai, L. M.; Gao, M.; Huang, S. M.; Mau, A. *J. Phys. Chem. B* **2001**, *105*, 618–622. (c) Dai, L. M. *Radiat. Phys. Chem.* **2001**, *62*, 55–68.
(11) Jorio, A.; Saito, R.; Hafner, J. H.; Lieber, C. M.; Hunter, M.; McClure, T.; Dresselhaus, G.; Dresselhaus, M. S. *Phys. Rev. Lett.* **2001**, *86*, 1118–1121.
(12) Chen, J.; Zhang, W. M.; Officer, D.; Swiegers, G. F.; Wallace, G. G. *Chem. Commun.* **2007**, 3353–3355.

JA105617Z